

Dephasing of resonant energy transfer in a cold Rydberg gas

W. R. Anderson,¹ M. P. Robinson,¹ J. D. D. Martin,² and T. F. Gallagher¹

¹Department of Physics, University of Virginia, Charlottesville, Virginia 22901

²Department of Physics, University of Waterloo, Waterloo, Ontario, Canada N2L 3G1

(Received 10 February 2002; published 5 June 2002)

When the dipole-dipole energy transfer, $\text{Rb } 25s_{1/2} + \text{Rb } 33s_{1/2} \rightarrow \text{Rb } 24p_{1/2} + \text{Rb } 34p_{3/2}$, resonant at fields of 3.0 and 3.4 V/cm, is observed in a cold Rydberg gas, the resonances are broader than expected for this dipole-dipole interaction alone. Using a variant of the Ramsey interference method, in which the system is detuned from the resonance, we observe a density-dependent dephasing which we attribute to the inhomogeneities in the always resonant dipole-dipole excitation exchange interactions $\text{Rb } 25s_{1/2} + \text{Rb } 24p_{1/2} \rightarrow \text{Rb } 24p_{1/2} + \text{Rb } 25s_{1/2}$ and $\text{Rb } 33s_{1/2} + \text{Rb } 34p_{3/2} \rightarrow \text{Rb } 34p_{3/2} + \text{Rb } 33s_{1/2}$. Since the dephasing rate is comparable to the observed widths, it appears that all of these interactions contribute to the observed linewidths.

DOI: 10.1103/PhysRevA.65.063404

PACS number(s): 32.80.Pj, 34.60.+z, 32.80.Rm

Recent resonant-energy-transfer experiments with cold Cs and Rb Rydberg atoms in magneto-optical traps (MOT's) have shown a behavior more like what is expected for an amorphous solid than for a gas [1–3]. Specifically, in normal vapors, even at temperatures as low as 1 K, resonant energy transfer occurs due to binary collisions between moving atoms [4,5]. In contrast, the cold atoms in a MOT are essentially motionless, so collisions are impossible. Rather, the static interactions between atoms are responsible for the energy transfer [1,2]. Furthermore, it appears that a given Rydberg atom no longer interacts with only one other atom, but with many other atoms at once. Here we present further evidence to show the importance of simultaneous multiple atom interactions.

The relevant energy levels for our experiment with Rb are shown in Fig. 1. At fields of 3.0 and 3.4 V/cm the energy-transfer process

$$25s_{1/2} + 33s_{1/2} \rightarrow 24p_{1/2} + 34p_{3/2} \quad (1)$$

is resonant, as shown in Fig. 1. There are two resonances corresponding to the two possible values of $|m_j|$ for the $34p_{3/2}$ state. If population is initially put into the $25s$ and $33s$ states, it can later be detected in the $34p$ and $24p$ states at the resonance fields of 3.0 and 3.4 V/cm, as shown in Fig. 2, a recording of the detected $34p$ population vs electric field. The process of Eq. (1) and Fig. 2 occurs due to dipole-dipole coupling between the two Rydberg atoms. The initial and final states of Eq. (1) are coupled with a strength given by $V = \mu\mu'/r^3$, where μ and μ' are the $25s$ - $24p$ and $33s$ - $34p$ dipole matrix elements, 284 and $73ea_0$, respectively, and r is the separation between the atoms. The dipole matrix elements were calculated using the Numerov algorithm as presented by Zimmerman *et al.* [6]. To simplify the notation, in the following discussion we shall use V as a shorthand label for the dipole-dipole interaction responsible for the energy transfer of Eq. (1).

When the widths of the observed energy-transfer resonances are compared to the strength of the resonant dipole-dipole interaction $V = \mu\mu'/r_0^3$ for a pair of atoms at the average spacing $r_0 = (4\pi N_0/3)^{-1/3}$, N_0 being the initial $25s$

and $33s$ number densities, the experimental widths are found to be much larger than $\mu\mu'/r_0^3$. For example, the energy-transfer resonances of Fig. 2, observed with a density of $25s$ and $33s$ atoms of $1.3 \times 10^9 \text{ cm}^{-3}$, are 6.8 MHz wide, but at this density $V = 0.11 \text{ MHz}$. Although a few atoms, of order 1%, are close enough to explain the observed widths, there are not enough of them to account for the magnitude of the observed population transfer, 15%. The proposed resolution of this apparent paradox is that there are two additional resonant-energy-transfer processes that need to be taken into account [1–3]:

$$25s_{1/2} + 24p_{1/2} \rightarrow 24p_{1/2} + 25s_{1/2} \quad (2)$$

and

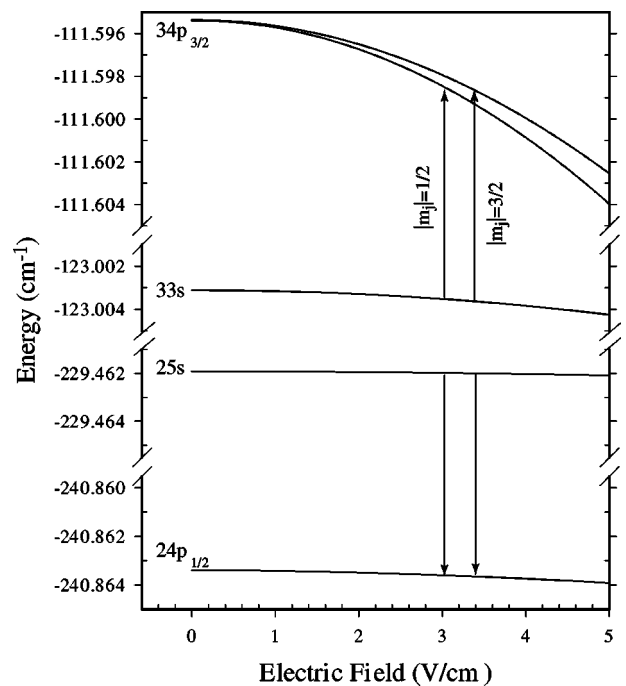


FIG. 1. Energy levels of the relevant states for ^{85}Rb in an electric field showing the resonant transitions at 3.0 and 3.4 V/cm.

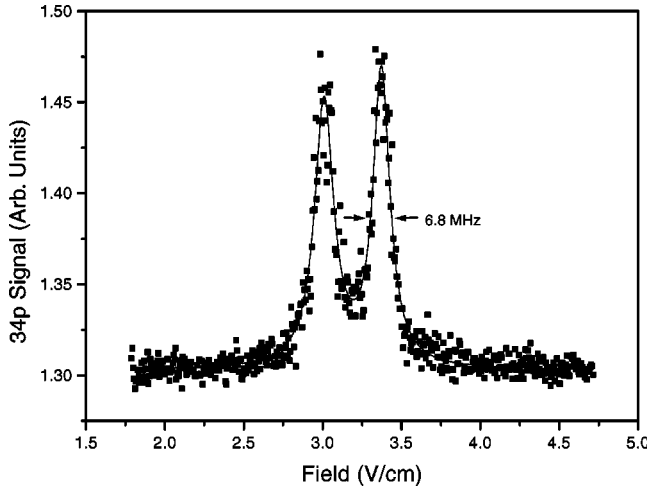


FIG. 2. Electric-field scan across the two resonances, with a density of $1.3 \times 10^9 \text{ cm}^{-3}$ in both the $25s$ and $33s$ Rydberg states. The full width half maximum of the $|m_j|=3/2$ resonance is 6.8 MHz. For small changes in field near the $|m_j|=3/2$ resonance the field-to-frequency conversion is 51 MHz/(V/cm).

$$33s_{1/2} + 34p_{3/2} \rightarrow 34p_{3/2} + 33s_{1/2}, \quad (3)$$

which are resonant at all electric fields, and proceed via dipole-dipole coupling of the initial and final states. The coupling strengths of the dipole-dipole interactions for these specific initial and final states are given by $\Gamma = \mu^2/r^3$ and $\gamma = \mu'^2/r^3$, respectively. As with V , we shall also use Γ and γ as shorthand labels for the dipole-dipole interactions responsible for the transfers of Eqs. (2) and (3). For reference, it is useful to note that at $25s$ and $33s$ densities of 10^9 cm^{-3} the values of V , Γ , and γ for a pair of atoms spaced by r_0 are 0.085, 0.329, and 0.022 MHz. All these interactions scale linearly with density. The simplest picture that accounts for the observed width and magnitude of the observed energy-transfer resonances is as follows. A small number of pairs of $25s$ and $33s$ atoms are close together and oscillate rapidly between the left- and right-hand sides of Eq. (1). The $24p$ and $34p$ population slowly diffuses away from these pairs by the resonant processes of Eqs. (2) and (3). This simple picture implicitly associates the rapid oscillation, and thus the observed widths of the resonances, with the energy transfer of Eq. (1) and the slow diffusion with Eqs. (2) and (3). Here we present evidence to support the notion that the dipole-dipole interactions responsible for Eqs. (2) and (3) contribute directly to the observed widths of the resonances and affect the population transfer from the initially populated $25s_{1/2}$ and $33s_{1/2}$ states. The measurements further underscore the fact that it is the simultaneous interaction among many atoms which is responsible for the observed energy-transfer. To be precise, we have done a variant of the Ramsey interference experiment [7] that effectively eliminates V , the dipole-dipole interaction responsible for Eq. (1), and shows the importance of the always-resonant interactions Γ and γ in the initial energy transfer.

The principle of the experiment is easily understood with a four-atom model. Consider four atoms, initially arranged as

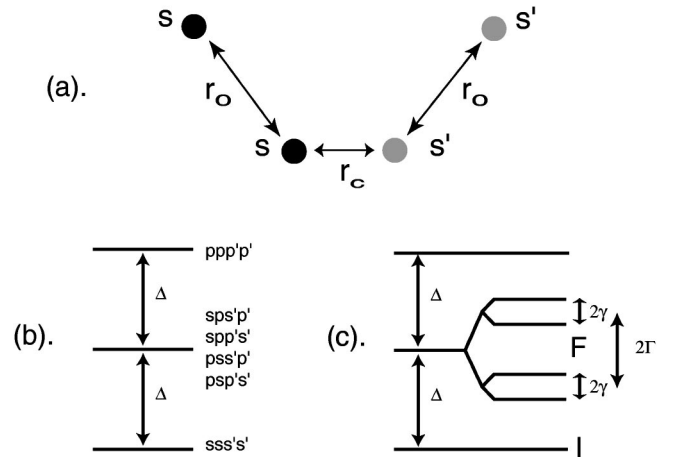


FIG. 3. (a) Four-atom model with one pair of atoms spaced by r_c and the others by r_0 , the average interatomic spacing. (b) Energy levels of the system with no dipole-dipole interactions. (c) Shifted energy levels after turning on the always-resonant interactions Γ and γ . The levels in the final state group F are coherent superpositions of the four intermediate energy levels in (b).

shown in Fig. 3(a), with two atoms in the $25s_{1/2}$ state and two in the $33s_{1/2}$ state. Two of the atoms are close together, spaced by r_c , and the others have the average spacing r_0 . In Fig. 3 we introduce the shorthand notation $s=25s$, $s'=33s$, $p=24p$, and $p'=34p$. We construct a direct product state, which is the product of the atomic wave functions for atoms at the four positions. The six relevant states are approximately degenerate. They are $sss's'$, $spp's'$, $sps'p'$, $pss'p'$, $psp's'$, $ppp'p'$, where the ordering denotes the position of the atoms from left to right in Fig. 3(a). Consider the case in which the energy transfer of Eq. (1) for a pair of atoms is far off resonance, by Δ . If we ignore the dipole-dipole interactions there are three energies as shown by Fig. 3(b), which reflect how many pairs of p and p' atoms there are. When we include the dipole-dipole interactions, V is unimportant since we are far off resonance. However Γ and γ are still important, and they lift the degeneracy of the middle group of states, as shown in Fig. 3(c).

Imagine that we excite Rb atoms to the $25s$ and $33s$ Rydberg states (s and s') in an off-resonant electric field. The atoms are then brought into the resonance of Eq. (1) twice with two temporally separated electric-field pulses, and population in the $34p$ state (p') is detected after the second field pulse as the time T between the pulses is varied. The electric-field pulses bring the atoms into resonance for the energy transfer of Eq. (1), so the electric-field pulses effectively turn on the interaction V . During the first pulse the dipole-dipole interaction V produces a coherent superposition of the initial state, labeled I in Fig. 3(c), and the group of intermediate states, labeled F in Fig. 3(c). Between the two pulses there is free evolution of the eigenstates of the superposition. During the second pulse the dipole-dipole interaction V drives the atoms toward F or back toward I , depending on the difference in the phase accumulation of the eigenstates between the pulses. Inspecting Fig. 3(c) we can see that if we ignore the weaker interaction γ there are two energy spacings $\Omega = \Delta \pm \Gamma$ between I and F , so we therefore

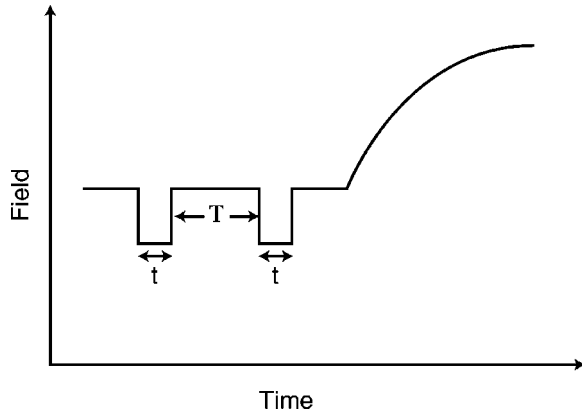


FIG. 4. Timing diagram for the Ramsey double field pulse and subsequent field ionization pulse. $T=0-50$ ns and $t=50$ ns.

expect two phase accumulations $(\Delta \pm \Gamma)T$ or two beat frequencies $\Delta \pm \Gamma$ in the observed signal. In reality there are not only four atoms, but many groups of atoms with different interatomic spacings. Accordingly, there is a range of values of Γ , and we do not expect to see two well defined frequencies $\Delta \pm \Gamma$ but a single frequency Δ that dephases at a rate which is some sort of average value of Γ . Note that Δ only depends on how far the static electric field is detuned from resonance, while the average value of Γ should be proportional to the density of $25s$ Rydberg atoms.

In the experiment, Rb atoms from a vapor are trapped in a MOT at a density of up to 5×10^{10} cm^{-3} . Roughly half are in the $5p_{3/2}$ state, and these are excited to the $25s_{1/2}$ and $33s_{1/2}$ Rydberg states with two pulsed lasers running at a 20-Hz repetition rate, producing maximum densities of 10^{10} cm^{-3} in each Rydberg state. The atoms are excited in a static field between 4.3 and 5.5 V/cm. At these fields the atoms are detuned from the resonance at 3.4 V/cm by 50 –

140 MHz, many times the observed linewidths of 2– 12 MHz. Two negative field pulses 50 ns long separated by time T are applied to bring the atoms into the resonance at 3.4 V/cm. Ideally we would like to make the field pulses as short as possible, but with pulses much shorter than 50 ns the resonances of Fig. 2 are not resolved, and the signal becomes vanishingly small. After the second field pulse, an ionizing field pulse is applied to ionize only the atoms in the $34p_{3/2}$ state. We detect the resulting ions with a dual microchannel plate detector and record the signal with a gated integrator as the time interval T is increased, as shown in Fig. 4.

In our description of the principle of the experiment we suggested that we expected to see a beat signal at the field-dependent frequency Δ , which decays at a density-dependent rate $1/\tau$. In Fig. 5 we show the interference signals for two different densities, 7.6×10^9 cm^{-3} and 1.9×10^9 cm^{-3} . The observed signals are fit to the form

$$S = A + B e^{-T/\tau} \cos(2\pi\Delta T), \quad (4)$$

i.e., to a constant offset and a decaying sinusoidal oscillation. We have measured the beat frequency for different detuning fields and compared it to the expected value, and, as shown in Fig. 6, the observed beat frequencies agree with the values calculated in the following way. We calculated the Stark shifts of the levels using the matrix diagonalization approach of Zimmerman *et al.* [6] and determined the polarizabilities of the four states involved. From these we have determined that the Stark shift of the $(33s + 25s) - (34p + 24p)$ interval is 7.5 MHz/(V/cm)². Using this Stark shift gives a zero field $(33s + 25s) - (34p + 24p)$ splitting of 88 MHz, so that the calculated beat frequency is given by

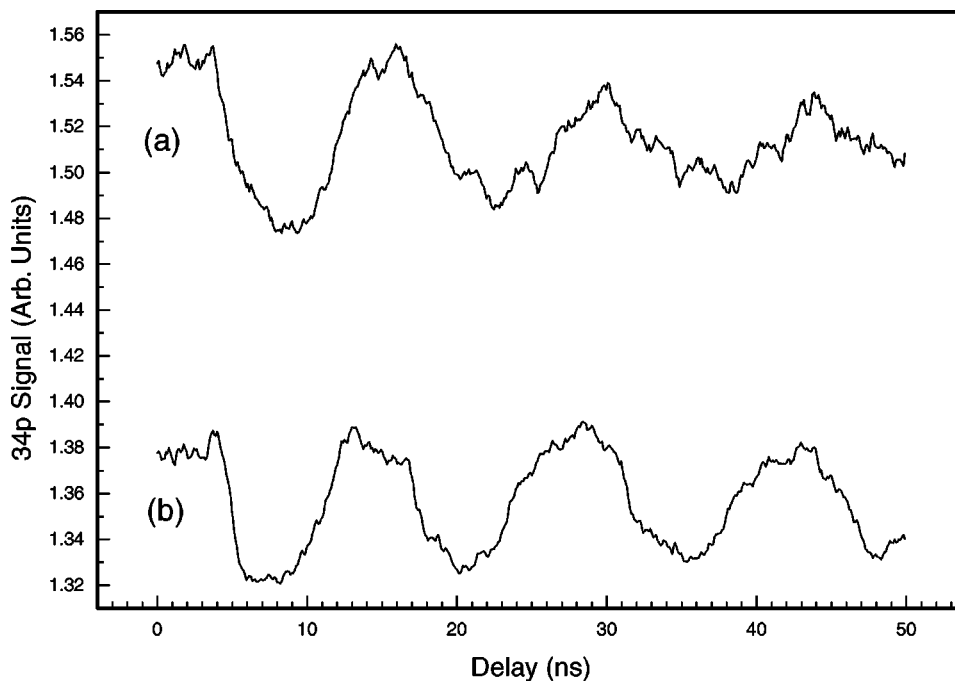


FIG. 5. Ramsey fringes showing dephasing for two densities: (a) 7.6×10^9 cm^{-3} ; (b) 1.9×10^9 cm^{-3} .

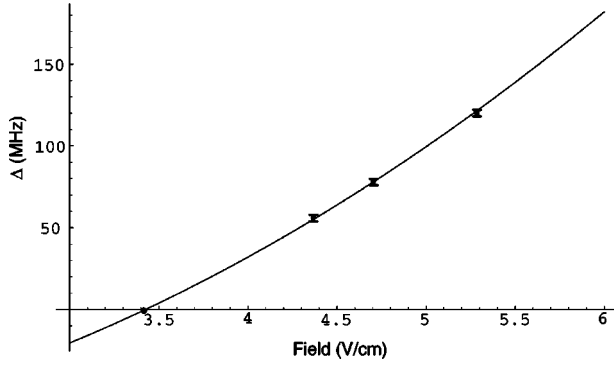


FIG. 6. The beat frequency Δ as a function of the field strength. The solid line indicates the calculated value, from Eq. (5), and the dots indicate measured values. The zero-frequency point comes from the resonant-energy-transfer resonance.

$$\Delta = (-88 \text{ MHz}) + \left(7.5 \frac{\text{MHz}}{(\text{V/cm})^2} \right) [F^2 (\text{V/cm})^2]. \quad (5)$$

There is no observable dependence of the beat frequency on the density of Rydberg atoms in the trap. While it is important that the beat frequency match the calculated value, it is the dependence of the decay rate of the beat signal on density which is of most interest, and as shown in Fig. 7, the decay rate is definitely density dependent. For the high- and low-density traces of Figs. 5(a) and 5(b), $1/\tau = 33.9 \times 10^6 \text{ s}^{-1}$ and $11.4 \times 10^6 \text{ s}^{-1}$, respectively.

If there were no other sources of dephasing, the dephasing rate should simply be due to Γ and γ , mostly to Γ since $\Gamma = 16\gamma$, and be proportional to the density. However, there are several complicating factors. There are several other sources of dephasing. Based on measurements made in higher electric fields, we estimate the electric-field inhomogeneities to be $\sim 1\%$, which should lead to inhomogeneous broadening of $\sim 0.15 \text{ MHz}$. Due to the trap's B field gradient of

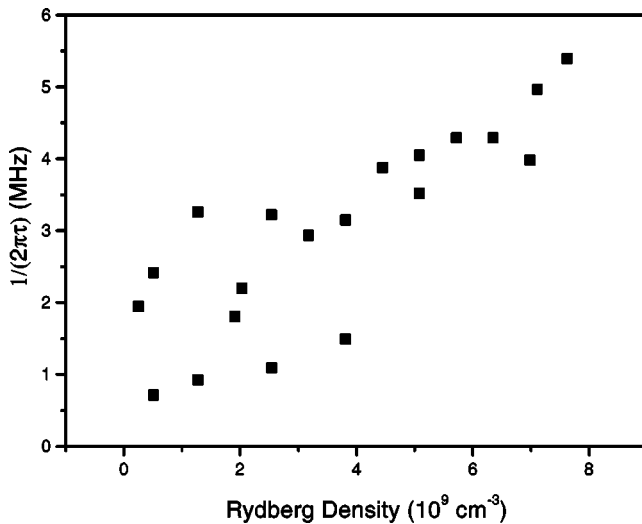


FIG. 7. Dephasing linewidth of the interference fringes as a function of the sum of the total population density in the $25s$ and $33s$ Rydberg states.

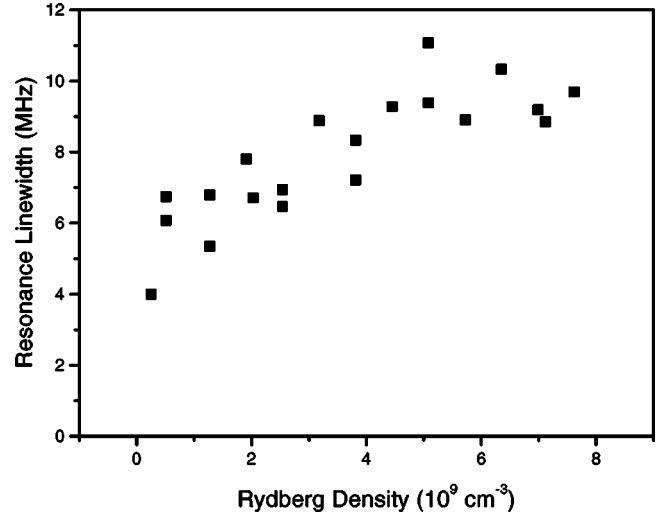


FIG. 8. The linewidth of the $|m_j|=3/2$ resonance as a function of the sum of the total population density in the $25s$ and $33s$ Rydberg states.

$\sim 10 \text{ G/cm}$, the magnetic field has an inhomogeneity of $\pm 1 \text{ G}$, and it is reasonable to expect linewidths of several megahertz from this source, as has recently been verified in microwave resonance experiments [8]. We note that the hyperfine splitting of the ^{85}Rb $25s$ state is 1.5 MHz [8,9], but it is presumably obscured by the inhomogeneous broadening described above. Although the broadening from these sources is not small, it is density independent, whereas dephasing due to Γ and γ is proportional to the $25s$ and $33s$ populations. Finally, we assume the atoms to be static, an assumption that is not good for the closest pairs of atoms.

We first measured the dephasing rate $1/\tau$ by varying the population in the trap, which allows us to nearly saturate the transitions to the $25s$ and $33s$ states, while holding the relative $25s$ and $33s$ populations constant. Since we are interested in comparing the dephasing rate $1/\tau$ to resonance linewidths, it is useful to express the dephasing rate in terms of $1/(2\pi\tau)$, i.e., as a frequency broadening. Following this convention, we show in Fig. 7 a plot of $1/(2\pi\tau)$ vs Rydberg atom density, which is the same for $25s$ and $33s$ states. There is a roughly linear density dependence, which extrapolates to a small dephasing rate at zero density, where the value of $1/(2\pi\tau)$ is compatible with the linewidths expected from the B field inhomogeneity. More important, the dephasing rate rises linearly with the number density, indicating that it is due to the dipole-dipole interactions Γ and γ (when the field is off-resonance, V does not contribute). Equally important, the linewidths associated with the dephasing are comparable to the observed linewidths of the resonances at the same density, as shown by Fig. 8, and we infer that the contributions of Γ and γ to the observed resonance widths are significant. Fitting lines to the points of Figs. 7 and 8 gives slopes of $0.5 \text{ MHz}/10^9 \text{ cm}^{-3}$ and $0.63 \text{ MHz}/10^9 \text{ cm}^{-3}$, respectively, which implies that about half the width comes from the omnipresent Γ and γ interactions.

Since $\Gamma = 16\gamma$ we expect most of the density dependence to come from the $25s$ density, and to verify this point we

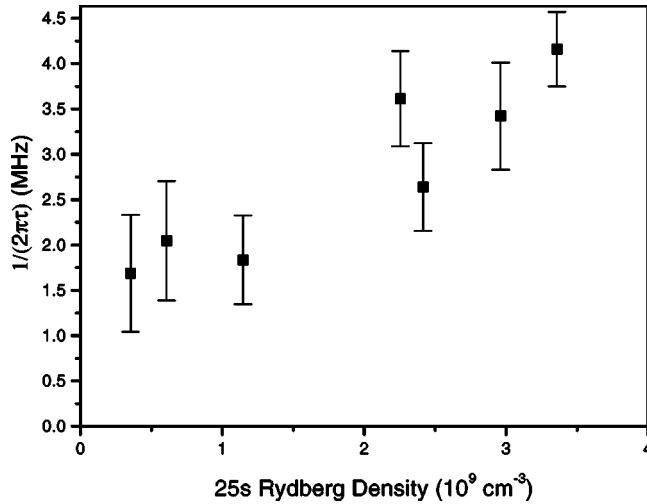


FIG. 9. Dephasing linewidth vs the 25s population density observed while holding the 33s population density constant at $4 \times 10^9 \text{ cm}^{-3}$.

have measured the dependence of the dephasing rate on the 25s and 33s densities independently. We first measured the dependence of the dephasing rate on the 25s density with the 33s density held constant at $4 \times 10^9 \text{ cm}^{-3}$, and there is a clear dependence of $1/(2\pi\tau)$ on the 25s density, as shown by Fig. 9. As in Fig. 7, the dephasing broadening extrapolated to zero 25s density is 1.3 MHz, indicating that the dephasing due to effects other than density-dependent dipole-dipole effects is small. The dephasing rate increases linearly with 25s density as expected, and the slope of Fig. 9 is $0.81 \text{ MHz}/10^9 \text{ cm}^{-3}$, twice the slope of Fig. 7, as expected if the dephasing is primarily due to Γ . The abscissa of Fig. 7 is the sum of the population densities in the 25s and 33s states.

Finally, we have measured the dependence of the dephasing rate on the 33s density, with the 25s density held constant at $4 \times 10^9 \text{ cm}^{-3}$. The results of these measurements are shown in Fig. 10. While the data are scattered, they are consistent with no dependence on the 33s density as expected

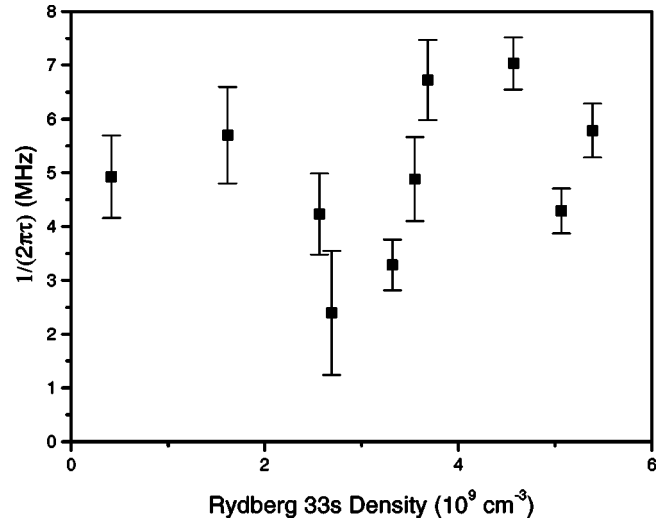


FIG. 10. Dephasing linewidth vs the 33s population density observed while holding the 25s population density constant at $4 \times 10^9 \text{ cm}^{-3}$.

from the fact that $\gamma = \Gamma/16$. Finally, we note that the slope of Figs. 7 and 9, $0.81 \text{ MHz}/10^9 \text{ cm}^{-3}$, is a factor of 2 larger than the value of Γ at a number density of 10^9 cm^{-3} , which gives us some confidence that the density dependence of $1/\tau$ does in fact come from the dipole-dipole interaction Γ of a $24p$ atom with several nearby 25s atoms.

In summary, by detuning far from resonance we have effectively turned off V , the interaction responsible for the energy transfer of Eq. (1), and have observed a density-dependent dephasing which we attribute to the spatial inhomogeneities in Γ . The dephasing rate is roughly comparable to the width of the observed energy-transfer resonance, which implies that the widths are due not only to the interaction V , but to Γ as well.

It is a pleasure to acknowledge discussions with V. Celli, J.S. Frasier, and P. Pillet during the course of this work, which has been supported by the Air Force Office of Scientific Research. M.P.R. gratefully acknowledges support from the AFRL Palace Knight Program.

-
- [1] I. Mourachko, D. Comparat, F. de Tomasi, A. Fioretti, P. Nosbaum, V.M. Akulin, and P. Pillet, Phys. Rev. Lett. **80**, 253 (1998).
 [2] W.R. Anderson, J.R. Veale, and T.F. Gallagher, Phys. Rev. Lett. **80**, 249 (1998).
 [3] J.S. Frasier, V. Celli, and T. Blum, Phys. Rev. A **59**, 4358 (1999).
 [4] R.C. Stoneman, M.D. Adams, and T.F. Gallagher, Phys. Rev. Lett. **58**, 1324 (1987).
 [5] D.S. Thomson, M.J. Renn, and T.F. Gallagher, Phys. Rev. Lett. **65**, 3273 (1990).
 [6] M.L. Zimmerman, M.G. Littman, M.M. Kash, and D. Kleppner, Phys. Rev. A **20**, 2251 (1979).
 [7] N.F. Ramsey, *Molecular Beams* (Oxford University Press, Oxford, 1985).
 [8] W. Li and I. Mourachko (private communication).
 [9] E. Arimondo, M. Inguscio, and P. Violino, Rev. Mod. Phys. **49**, 31 (1977).